SCIENCE CHINA
Physics, Mechanics & Astronomy

• Research Paper •

May 2011 Vol.54 No.5: 923–929
doi: 10.1007/s11433-011-4302-4

Probe stiffness regulates receptor-ligand bond lifetime under force†

ZHANG Yan[1,2], LÜ ShouQin[1,2] & LONG Mian[1,2*]

[1] *Key Laboratory of Microgravity, Institute of Mechanics, Chinese Academy of Sciences, Beijing 100190, China;*
[2] *National Microgravity Laboratory and Center of Biomechanics and Bioengineering, Institute of Mechanics, Chinese Academy of Sciences, Beijing 100190, China*

Received April 19, 2010; accepted July 30, 2010; published online March 14, 2011

Receptor-ligand bond dissociation under applied force is crucial to elucidate its biological functionality when the molecular bond is usually connected to a mechanical probe. While the impact of probe stiffness, k, on bond rupture force has recently attracted more and more attention, the mechanism of how it affects the bond lifetime, however, remains unclear. Here we quantified the dissociation lifetime of selectin-ligand bond using an optical trap assay with low stiffness ranging from 3.5×10^{-3} to 4.7×10^{-2} pN/nm. Our results indicated that bond lifetime yielded distinct distributions with different probe stiffness, implying the stochastic feature of bond dissociation. It was also found that the mean lifetime varied with probe stiffness and that the catch bond nature was visualized at $k\geqslant3.0\times10^{-2}$ pN/nm. This work furthered the understanding of the forced dissociation of selectin-ligand bond at varied probe stiffness, which is physiologically relevant to the tethered rolling of leukocytes under blood flow.

probe stiffness, bond lifetime, optical trap

PACS: 82.37.Np, 87.15.Kg, 87.80.Cc

1 Introduction

Receptor-ligand interactions, usually named a "lock-and-key" model, are crucial to many biological processes such as inflammatory cascade and tumor metastasis [1–5]. For example, a P-selectin receptor expressed on the activated endothelial cell or platelet tends to form a molecular bond with its P-selectin glycoproetein ligand 1 (PSGL-1) expressed on the microvillus tip of flowing neutrophil, which initiates the leukocyte rolling over and tethering onto the endothelium under blood flow [6,7]. This physiological process turns to be a forced association and dissociation dynamics of receptor-ligand bond. To elucidate the underlying mechanisms involved requires theoretical modeling and experimental quantification of bond formation and dissociation using the approach that coordinates biological, mechanical, and chemical rationale.

Theoretically, a few models have been proposed to determine how mechanical forces affect bond dissociation. For example, bond reverse rate (in s^{-1}) was assumed to reduce (Bell model [8]) or enhance (Dembo model [9]) exponentially with applied forces, suggesting that the bond lifetime (defined as the reciprocal of reverse rate at that force) exhibits the biphasic transition between slip bond [8] and catch bond [9]. A dynamic force spectroscopy theorem was further developed, upon the Bell model, to formulate the rupture force dependence on the logarithm of loading rate (defined as the product of probe stiffness and retract velocity; in pN/s) [10]. Two working modes, *i.e.*, lifetime mode at the constant applied force and rupture force mode at a constant loading rate, were then proposed upon these theoretical predictions to map the bond lifetime and rupture force, respectively.

Experimentally, various assays have been used to test the

*Corresponding author (email: mlong@imech.ac.cn)
† Contributed by Long Mian

forced bond dissociation including atomic force microscopy or AFM [11–15] and optical trap or OT [16,17]. Using an AFM approach, for example, the existence of catch bond was first visualized from the forced bond lifetime [18], and the bond rupture force dependence on physical factors (approaching velocity and contact duration between the receptor and the ligand pair) [13] and on force history (reverse rate as a single value function of force) [15] were well determined for the forced dissociation of P-selectin-PSGL-1 bond. Recently, we applied an OT approach to quantify the probe stiffness dependence of bond dissociation [17] and found that the rupture force of P-selectin-PSGL-1 bond is stiffness-dependent. Such new observations, as compared to those for loading rate dependence of rupture force [10], implied that there might exist distinct mechanisms of bond lifetime when the probe is connected to the molecular bond.

Here the force dependence of bond lifetime was further quantified using the OT assay. A constant force mode was employed to determine the probe stiffness dependence of bond lifetime at the same loading rate. The impact of force history was also tested to elucidate if the bond lifetime is a single value function of applied force.

2 Materials and methods

2.1 Proteins and antibodies

PSGL-1 was purified from human neutrophils following a modified protocol, and the purity of the proteins was analyzed by SDS-PAGE on 7.5% polyacrylamide gels followed by silver staining [19]. Soluble P-selectin consisting of Lec-EGF domains plus nine CRs but with no transmembrane and cytoplasmic domains [20], anti-P-selectin capturing (S12) and blocking (G1) monoclonal antibodies (mAbs) [19], and anti-PSGL-1 capturing (PL2) and blocking (PL1) mAbs [21] were generous gifts from Dr. MCEVER Rodger P. (Oklahoma Medical Research Foundation). FITC-conjugated goat anti-mouse secondary mAbs and bovine serum albumin (BSA) were purchased from Sigma (St. Louis, MO).

2.2 Functionalized microbeads

The protocol to functionalize the microbeads was described previously [17]. Briefly, 2.32 μm- and 5.66 μm-diameter silica microbeads (Bangs Lab, Fishers, IN) were incubated overnight at 4°C in 10 μg/ml capturing mAbs S12 and PL2, respectively. After being washed three times with phosphate buffer solution (PBS), the microbeads were incubated by 2% BSA to block nonspecific adhesions for 12 hours and then incubated with 15 ng/ml P-selectin and PSGL-1 for 12 hours, respectively. After being rinsed with PBS and being re-blocked with 2% BSA, P-selectin- and PSGL-1-coupled microbeads were ready for measurements.

2.3 Site density determination

Site densities of surface proteins coated on microbeads were determined using flow cytometry and immunoradiometric assay as described previously [20,22,23]. In short, for measuring the densities of S12 and PL2 so adsorbed, one set of S12- or PL2-coated microbeads was incubated with FITC-conjugated goat anti-mouse mAbs at a concentration of 10 μg/ml in PBS on ice for 45 min. After being washed three times with phosphate buffer solution (PBS), the microbeads were analyzed by a flow cytometer (BD Biosciences, San Jose, CA). Site densities were then calculated by comparing the fluorescence intensities of the silica microbeads with those of standard beads (Bangs, Fishers, IN) [24]. Another set of S12- or PL2- coated microbeads was incubated with the corresponding P-selectin or PSGL-1 and the site density of P-selectin or PSGL-1 was measured by immunoradiometric assay [20]. A calibration curve was obtained for each protein by plotting the protein site density against the mean fluorescence intensity of the capturing mAb (data not shown) to allow calculation of the site densities of selectin or PSGL-1 from the mean fluorescence intensities of the capturing mAb. To obtain the infrequent binding events mediated by single P-selectin-PSGL-1 bond, the site densities of both proteins were adjusted to reach the low adhesion probability less than 25% [24].

2.4 Optical trap assay

The set-up of an optical trap assay was described previously [17]. In brief, a floating 2.32 μm-diameter microbead coupled with P-selectin was trapped optically while a 5.66 μm-diameter PSGL-1-coupled microbead was immobilized on the substrate. The immobilized microbead was brought by the piezo stage (PZT) to make contact with the P-selectin-coupled microbead (Figure 1(a)). The approach velocity, contact duration, and retract velocity were controlled using a custom user interface. Real time images of microbead movement were recorded by a CCD camera with a spatial and temporal resolution of 125 nm/pixel and 40 ms/frame for off-line analysis. Cross-correlation method [25] was used to determine the off-center displacement of the P-selectin-coupled microbead from the trap center with an accuracy of ~2 nm along the x- and y-axes. Spring constant k of the trap was determined using the Stokes law [26], which spans from 3.5×10^{-3} to 47.0×10^{-3} pN/nm upon varied laser power. All the measurements were done at room temperature (26 ± 1°C).

2.5 Bond lifetime measurements

For lifetime measurements, an immobilized PSGL-1-coupled microbead was brought by a piezo stage (PZT) to make contact with the trapped P-selectin-coupled microbead for 2 s and then retracted at a given loading rate. The PZT

stopped once it had arrived at a predetermined distance to apply a constant force (f=k×d) to the bond. The lifetime was measured from the instant when the PZT stopped to the instant when the bond fails (Figure 1(b)). Such an approach-contact-retract cycle was repeated more than 200 times in each loading set to collect the ensemble data of lifetime from bond-formed events. At a given loading rate of 10 pN/s, seven pairs of systematically-varied spring constant and retract velocity were used for lifetime measurements, and 41–83 lifetimes were obtained for each set. The rupture force mode was also employed here for binding specificity tests (Figure 1(c)).

2.6 Mechanokinetic theory and data analysis

Data for bond dissociation were analyzed using a first-order irreversible unbinding kinetics,

$$\ln P_b(t) = -k_r(f)t, \tag{1a}$$

$$P_b(0) = 1, \tag{1b}$$

where $P_b(t)$ is the probability of having a bond at time 0 to remain bound at time t, and $k_r(f)$ is the reverse rate of a bond at force f. For lifetime measurements, the time dependence of $P_b(t)$ and $k_r(f)$ can be transformed to:

$$\ln[(\text{Number of bonded event of } t_i \geqslant t)/(\text{Total bonded events})] = -k_r(f)t. \tag{2}$$

Thus, the −1/slope of the plot of ln(Number of bonded event of $t_i \geqslant t$) against t yields $k_r(f)$. For first-order dissociation kinetics, −1/slope is equal to the mean lifetime $\langle t\rangle$ and standard deviation of lifetime $\sigma(t)$ [18]:

$$\langle t\rangle = \int_0^\infty t\,\mathrm{d}(1-P_b(t)) = -\int_0^\infty t\,\mathrm{d}\exp(-k_r(f)t) = 1/k_r(f), \tag{3}$$

$$\sigma^2(t) = \int_0^\infty (t-\langle t\rangle)^2\,\mathrm{d}(1-P_b(t)) = 1/k_r^2(f) \Rightarrow \sigma(t) = 1/k_r(f). \tag{4}$$

Lifetimes measured at forces ranging from 1 to 17 pN were divided into lifetime bins with bin size of 0.2 s and analyzed using the mean lifetime $\langle t\rangle$ (eq. 3).

3 Results

3.1 Binding is specific

The adhesion frequency measured at an approaching veloc-

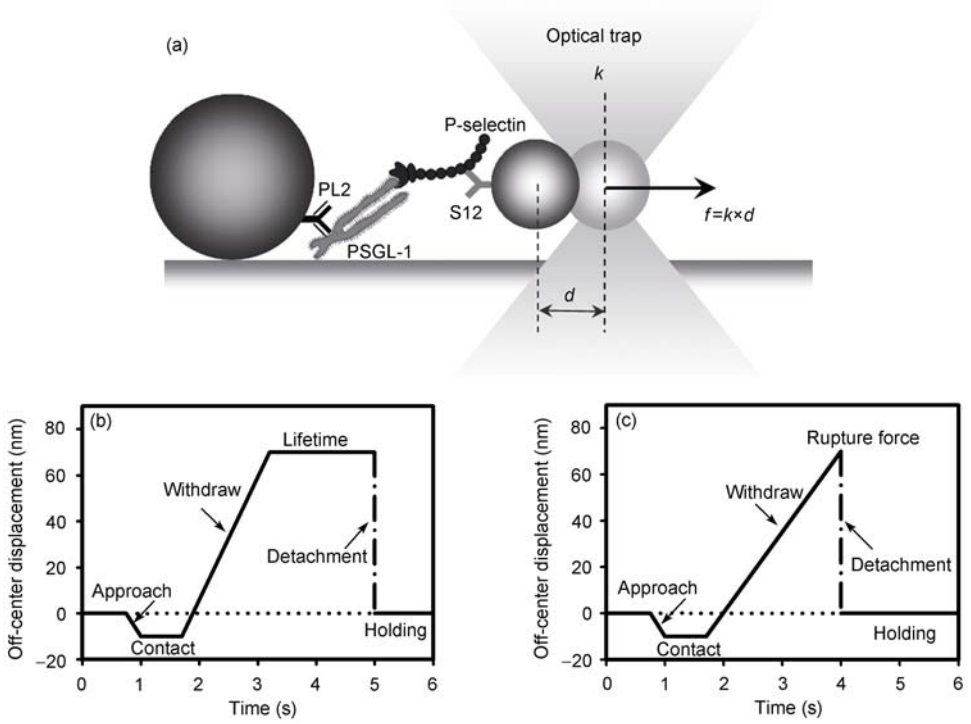

Figure 1 Optical trap set-up and experimental procedure. (a) Illustration of a functionally-coated molecule pair. P-selectin was coupled via pre-coated capturing mAb S12 onto a 2.32 μm-diameter microbead, and PSGL-1 was coupled via pre-coated capturing mAb PL2 onto a 5.66 μm-diameter microbead. P-selectin-coupled microbead was held in a trap and brought into contact with PSGL-1-coupled microbead to form a selectin-ligand bond. (b) Typical time course of the off-center displacement for rupturing P-selectin-PSGL-1 bond using lifetime mode and (c) rupture force mode. P-selectin-coupled microbead was driven to approach, contact, and retract from PSGL-1-coupled microbead, and was bounced back to the trap center when the bond dissociated.

ity of 500 nm/s, a retracting velocity of 1000 nm/s and a contact time of 2 s was used to quantify the specific bindings between P-selectin- and PSGL-1-coupled microbeads. Here the frequency is calculated as the fraction of adhesive events from a total of 1000 test cycles. As exemplified in Figure 2(a), the adhesion was mediated by specific P-selectin-PSGL-1 interactions, because 20%–25% of adhesion frequency was observed when P-selectin-coated 2.32 μm microbead contacted to PSGL-1-coated 5.66 μm microbead but it was reduced to 5%-10% when P-selectin or PSGL-1 constructs were absent. In addition, the adhesion was blocked by mAbs against PSGL-1 (PL1), P-selectin (G1), and by the calcium chelator EDTA. It was also pointed out that >80% of binding events measured are single-bond events when the site densities of interacting molecules were adjusted to have the adhesion frequency of <25% (Figure 2(a)) [22–24,27]. Taken together, the adhesions between two microbeads were specifically mediated, most likely, by single binding event of P-selectin and PSGL-1 pair.

To further test whether the adhesion between two microbeads was mediated by irreversible interaction of P-selectin-PSGL-1 bond, a running frequency test was performed

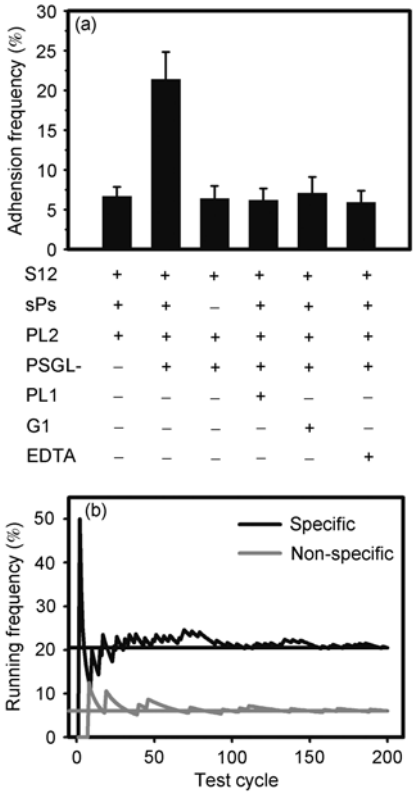

Figure 2 Binding specificity. (a) Adhesion frequency was obtained from 10 pairs of P-selectin- and PSGL-1-coated microbeads with 100 contacts each pair at contact duration of 2 s. Data was presented as the mean ± SD; (b) running frequency was obtained from 200 contacts of two interacting microbeads coated with P-selectin- and PSGL-1 pair (black line) or non-specific BSA proteins (grey line).

to get the dependence of adhesion frequency on test cycle N (=200). As exemplified in Figure 2(b), the adhesion frequency fluctuated dramatically at the first test cycles and tended to be stabilized with the following test cycles when both the P-selectin and PSGL-1 molecules were present, which was much higher than that when the two microbeads were coated with BSA proteins.

3.2 Lifetime makes different distribution at the same applied force and loading rate

To understand the impact of probe stiffness on the bond lifetime of P-selectin-PSGL-1 interactions at low loading rates, seven combinations of stiffness, k=(3.5, 5.0, 7.3, 8.7, 20.0, 30.0 and 47.0)×10^{-3} pN/nm together with respective retract velocities, v=2857, 2000, 1369, 1149, 500, 333 and 212 nm/s were used to retain the same loading rate of 10 pN/s. As exemplified in Figure 3, the bond lifetime under a given applied force exhibited a single peak at each combination, but was distributed differently with varied stiffness, which indicates that the bond dissociation depends on both stiffness and retract velocity even at the same loading rate. At a given applied force of 5 and 7 pN, for example, the bond lifetime at very low stiffness ($k\leqslant 5.0\times10^{-3}$ pN/nm) was distributed much broader than those at relatively high stiffness (k=7.3 and 8.7×10^{-3} pN/nm), whereas it became further broadened with increased stiffness when $k\geqslant 2.0\times10^{-2}$ pN/nm (Figures 3(a) and 3(b)). Similar data were obtained when the applied force was set to be the high values of 15 and 17 pN (Figure 3(c) and 3(d)).

This dependence was further tested by plotting the mean lifetime against the applied force (Figure 4(a)). It is evident that the mean lifetime $\langle t\rangle$ is not a single-value function of applied force. At the same applied force, for example, the mean lifetime $\langle t\rangle$ varied dramatically from 0.19 to 0.64 s (f = 1 pN) or from 0.49 to 0.87 s (f=15 pN). And at the similar lifetime so measured (*i.e.*, $\langle t\rangle$ = 0.06 s), the applied force was altered by more than one order-of-magnitude from 1 to 11 pN. These results indicated that not a unique lifetime spectrum is able to be obtained at a given loading rate when probe stiffness and retract velocity are systematically varied. Moreover, although the mean lifetime at $f\leqslant 10$ pN exhibited the randomness with the stiffness, it tended to rise with increased stiffness at the same applied force when $f>10$ pN.

3.3 Probe stiffness regulates bond dissociation at low loading rates

To isolate the impact of probe stiffness on forced dissociation of P-selectin-PSGL-1 bonds, the retract velocity was systematically varied from 2857 to 212 nm/s at a given stiffness k ranging from 3.5×10^{-3} to 4.7×10^{-2} pN/nm. As exemplified in Figure 4(b), mean lifetimes fluctuated ran-

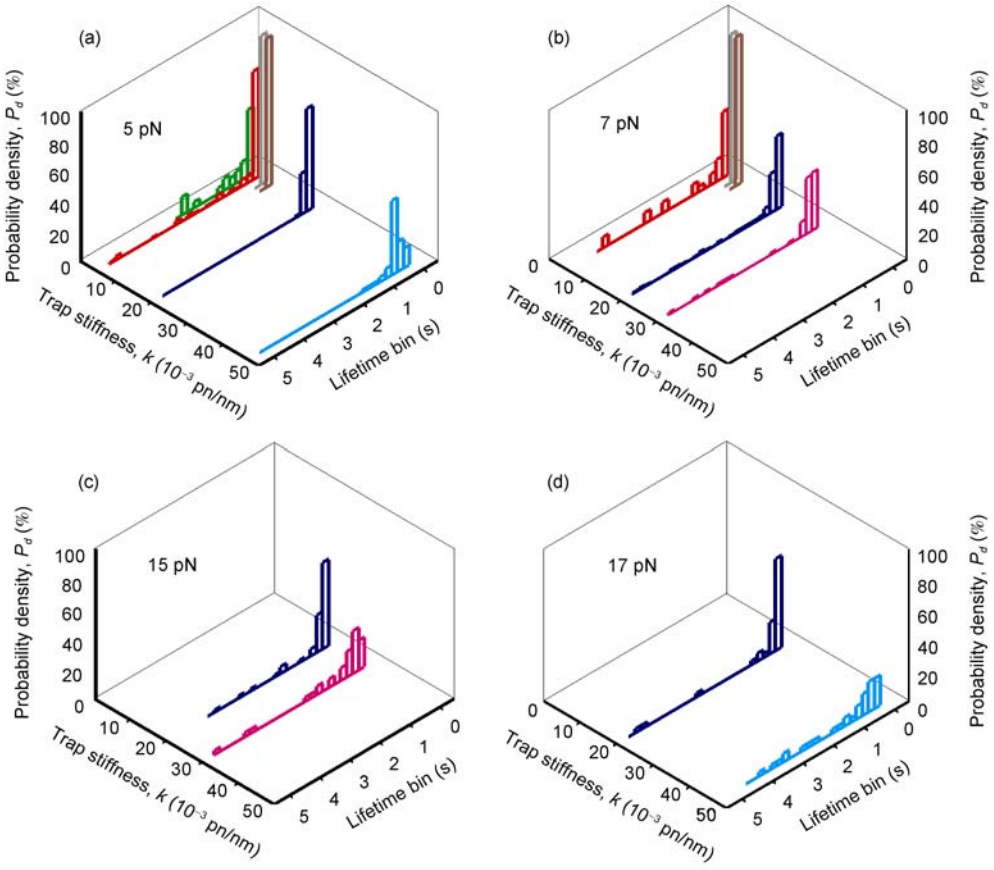

Figure 3 Dependence of the lifetime distribution on probe stiffness at a loading rate of 10 pN/s. Histograms of lifetimes measured were plotted against the stiffness at the same applied force of f=5 (a), 7 (b), 15 (c), and 17 pN (d). Seven stiffness of k=3.5 (green), 5.0 (red), 7.3 (gray), 8.7 (dark-red), 20.0 (blue), 30.0 (pink), and 47.0×10^{-3} pN/nm (cyan) were adjusted to a given loading rate of 10 pN/s in lifetime measurements at each applied force.

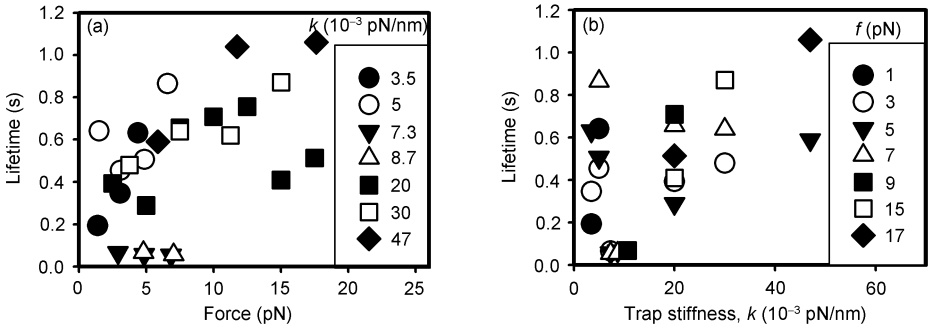

Figure 4 Dependence of mean lifetime on applied force (a) and probe stiffness (b). (a) Plotted was the mean lifetime against f at the stiffness of k=3.5 (solid circles), 5.0 (open circles), 7.3 (solid downwards-triangles), 8.7 (open upwards-triangles), 20.0 (solid squares), 30.0 (open squares), and 47.0×10^{-3} pN/nm (solid diamonds); (b) Plotted was the mean lifetime against k at the applied force of f=1 (solid circles), 3 (open circles), 5 (solid downwards-triangles), 7 (open upwards-triangles), 9 (solid squares), 15 (open squares), and 17 pN (solid diamonds). Error bars are not shown for clarity.

domly with applied force when $k \leqslant 2.0\times10^{-2}$ pN/nm, i.e., $\langle t \rangle$ = 0.39, 0.29, 0.66, 0.71, 0.41 and 0.51 s when f=3, 5, 7, 9, 15, and 17 pN, respectively, at low k=2.0×10^{-2} pN/nm. These data proposed the stochastic nature of spontaneous dissociation of P-selectin-PSGL-1 bonds, which is in agreement with what we had observed previously using the rupture force mode [17]. At high k=3.0 and 4.7 × 10^{-2} pN/nm, however, the mean lifetime appeared to be enhanced with increased applied force ranging from 3 to 15 pN and from 5 to 17 pN, respectively, implying that the P-selectin- PSGL-1 bonds behaved like a catch bond. Together, these results suggest that the presence of catch bond is associated with the stiffness of the mechanical probe applied.

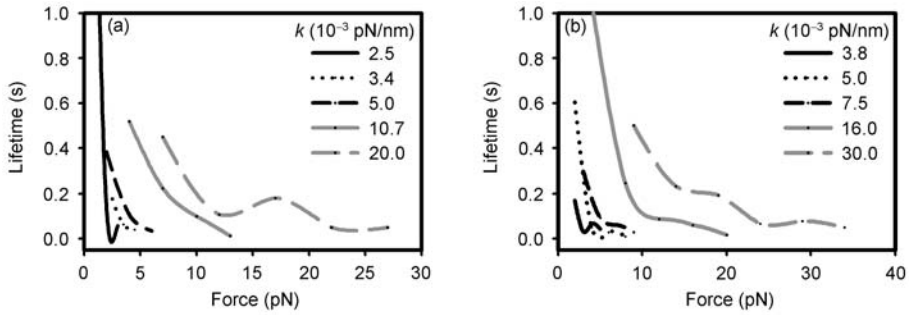

Figure 5 Force dependence of bond lifetime estimated from measured rupture force data [17] at a loading rate of 10 (a) or 15 pN/s (b).

4 Discussion

The goal of the current work is to elucidate the biophysical mechanisms of forced dissociation of receptor-ligand bond at varied probe stiffness. In contrast to most of the existing work that deals with bond rupture force, here we focused on quantifying the bond lifetime when a soft probe is connected to the selectin-ligand bond. Our results indicate that the bond lifetime distribution is sensitive to the probe stiffness applied at the same loading rate (Figure 3) and that the force dependence of bond lifetime is stiffness-dependent (Figures 4(a) and 4(b)). This observation is in excellent agreement with the previous findings in our and other labs that the probe stiffness regulates the bond dissociation at varied force applications [17].

It has been noticed that the bond lifetime at a force is able to be predicted from rupture force data at a given loading rate [15]. Such a prediction relies on the employed model of mechanokinetic coupling and the pre-requite assumption of a single-valued, instantaneous, and history-free dependence of applied force on the reverse rate, which results in a model-dependent lifetime estimation. Direct bond lifetime measurements, although unable to extract the zero-force reverse rate and energy landscape parameters, result in the model-free lifetime data. Here only the assumption that the reverse rate of bond dissociation is a single-value function of external force should be satisfied, which is quite applicable in many receptor-ligand systems. As illustrated in the force dependence of lifetime that was estimated from measured rupture force data [17] at loading rates of 10 (Figure 5(a)) and 15 pN/s (Figure 5(b)), the catch bond feature tended to disappear, presumably due to the model-dependent prediction. It should be pointed out that, although the bond lifetime determination is not model-dependent, it is still force-history dependent since distinct responses of a molecular bond are found to different loading pathways.

Such stiffness dependence of bond lifetime also provides the biophysical bases for understanding physiological functions of selectin-ligand interactions. For a leukocyte rolling over and tethering onto the endothelium, applying an external force via blood flow on a receptor-ligandbond is conceptually like pulling the bond complex using a mechanical probe that mimics the compliant nature of cytoplasmic structures attached to the binding site [28]. The stiffness of microvillus on which PSGL-1 expressed is 4.3×10^{-2} pN/nm or much less if the microvillus is extended under blood flow to form a long thin membrane cylinder (tether) [29], implying that the tethered dissociation is associated with the stiffness of microvillus. The data presented here validated the hypothesis that the bond lifetime is dependent on the probe stiffness. It also indicated that the catch bond behavior of P-selectin-PSGL-1 bond is strongly stiffness-dependent (Figure 4(b)). These results proposed an alternative mechanokinetic mechanism in mediating leukocytes rolling under blood flow.

In conclusion, we used an optical trap approach to visualize directly bond dissociation at low probe stiffness and loading rates. Weak force dependence of bond lifetime was found at very low probe stiffness ($\leqslant2.0\times10^{-2}$ pN/nm), suggesting the stochastic nature of spontaneous dissociation of selectin-ligand bond. The catch bond feature became visible at relatively high stiffness ($\geqslant3.0\times10^{-2}$ pN/nm), indicating that the bond lifetime tends to be gradually regulated by external forces. These results further the understandings of the regulating mechanisms of probe stiffness on bond dissociation (especially for the stiffness dependence of the presence of catch bond).

This work was supported by the National Natural Science Foundation of China (Grant Nos. 10902117, 10702075, 30730032 and 11072251), Chinese Academy of Sciences (Grant Nos. KJCX2-YW-L08 and Y2010030), and the National Key Basic Research Foundation of China (Grant No. 2011CB710904). The authors are grateful to Dr. MCEVER Rodger P. (Oklahoma Medical Research Foundation) for generous gifts of P-selectin, S12, G1, PL2, and PL1 proteins, to Dr. Ye ZhiYi (Chongqing University) for PSGL-1 purification, and to Dr. Sun Ganyun for technical assistance.

1 Lawrence M B, Springer T A. Leukocytes roll on a selectin at physiological flow-rates: Distinction from and prerequisite for adhesion through integrins. Cell, 1991, 65: 859–873
2 McEver R P. Adhesive interactions of leukocytes, platelets, and the vessel wall during hemostasis and inflammation. Thromb Haemostasis, 2001, 86: 746–756
3 McEver R P. Selectins: Lectins that initiate cell adhesion under flow. Curr Opin Cell Biol, 2002, 14: 581–586

4 Springer T A. Adhesion receptors of the immune system. Nature, 1990, 346: 425–434
5 Springer T A. Traffic signals for lymphocyte recirculation and leukocyte emigration: The multistep paradigm. Cell, 1994, 76: 301–314
6 Li F G, Erickson H P, James J A, et al. Visualization of P-selectin glycoprotein ligand-1 as a highly extended molecule and mapping of protein epitopes for monoclonal antibodies. J Biol Chem, 1996, 271: 6342–6348
7 Moore K L, Stults N L, Diaz S, et al. Identification of a specific Glycoprotein ligand for P-Selectin (Cd62) on myeloid cells. J Cell Biol, 1992, 118: 445–456
8 Bell G I. Models for specific adhesion of cells to cells. Science, 1978, 200: 618–627
9 Dembo M, Torney D C, Saxman K, et al. The reaction-limited kinetics of membrane-to-surface adhesion and detachment. Proc R Soc London B, 1988, 234: 55–83
10 Evans E, Ritchie K. Dynamic strength of molecular adhesion bonds. Biophys J, 1997, 72: 1541–1555
11 Fritz J, Katopodis A G, Kolbinger F, et al. Force-mediated kinetics of single P-selectin ligand complexes observed by atomic force microscopy. Proc Natl Acad Sci USA, 1998, 95: 12283–12288
12 Hanley W, McCarty O, Jadhav S, et al. Single molecule characterization of P-selectin/ligand binding. J Biol Chem, 2003, 278: 10556–10561
13 Lü S Q, Ye Z Y, Zhu C, et al. Quantifying the effects of contact duration, loading rate, and approach velocity on P-selectin-PSGL-1 interactions using AFM. Polymer, 2006, 47: 2539–2547
14 Marshall B T, McEver R P, Zhu C. Mechanical properties of the P-selectin/PSGL-1 interaction. In: Proceedings of Second Joint Embs-Bmes Conference, 2002. Vols 1-3, 337–338
15 Marshall B T, Sarangapani K K, Lou J Z, et al. Force history dependence of receptor-ligand dissociation. Biophys J, 2005, 88: 1458–1466
16 Rinko L J, Lawrence M B, Guilford W H. The molecular mechanics of P- and L-selectin lectin domains binding to PSGL-1. Biophys J, 2004, 86: 544–554
17 Zhang Y, Sun G Y, Lü S Q, et al. Low spring constant regulates p-selectin-psgl-1 bond rupture. Biophys J, 2008, 95: 5439–5448
18 Marshall B T, Long M, Piper J W, et al. Direct observation of catch bonds involving cell-adhesion molecules. Nature, 2003, 423: 190–193
19 Geng J G, Bevilacqua M P, Moore K L, et al. Rapid neutrophil adhesion to activated endothelium mediated by GMP-140. Nature, 1990, 343: 757–760
20 Ushiyama S, Laue T M, Moore K L, et al. Structural and functional-characterization of monomeric soluble P-Selectin and comparison with membrane P-Selectin. J Biol Chem,1993, 268: 15229–15237
21 Moore K L, Patel K D, Bruehl R E, et al. P-Selectin Glycoprotein Ligand-1 Mediates Rolling of Human Neutrophils on P-Selectin. J Cell Biol, 1995, 128: 661–671
22 Huang J, Chen J, Chesla S E, et al. Quantifying the effects of molecular orientation and length on two-dimensional receptor-ligand binding kinetics. J Biol Chem, 2004, 279: 44915–44923
23 Wu L, Xiao B T, Jia X L, et al. Impact of carrier stiffness and microtopology on two-dimensional kinetics of P-selectin and P-selectin glycoprotein ligand-1 (PSGL-1) interactions. J Biol Chem, 2007, 282: 9846–9854
24 Chesla S E, Selvaraj P, Zhu C. Measuring two-dimensional receptor-ligand binding kinetics by micropipette. Biophys J, 1998, 75: 1553–1572
25 Gelles J, Schnapp B J, Sheetz M P. Tracking kinesin-driven movements with nanometre-scale precision. Nature, 1988, 331: 450–453
26 Ghislain L P, Switz N A, Webb W W. Measurement of small forces using an optical trap. Rev Sci Instrum, 1994, 65: 2762–2768
27 Long M, Zhao H, Huang K S, et al. Kinetic measurements of cell surface E-selectin/carbohydrate ligand interactions. Annu Biomed Eng, 2001, 29: 935–946
28 Evans E A, Calderwood D A. Forces and bond dynamics in cell adhesion. Science, 2007, 316: 1148–1153
29 Shao J Y, Ting-Beall H P, Hochmuth R M. Static and dynamic lengths of neutrophil microvilli. Proc Natl Acad Sci, 1998, 95: 6797–6802